Inorg. Chem. **2009**, *48*, 3125−3131

Inorganic Chemistry
Article

Mononuclear Mn^{III} and Mn^{IV} Bis-terpyridine Complexes: Electrochemical Formation and Spectroscopic Characterizations

Sophie Romain, Carole Baffert,[†] Carole Duboc, Jean-Claude Leprêtre,[‡] Alain Deronzier,[*] and Marie-Noëlle Collomb[*]

Université Joseph Fourier Grenoble 1/CNRS, Département de Chimie Moléculaire, UMR-5250,
Institut de Chimie Moléculaire de Grenoble FR- CNRS-2607, BP-53,
38041 Grenoble Cedex 9, France

Received December 23, 2008

The electrochemical behavior of two mononuclear Mn^{II} bis-terpyridine complexes, $[\mathrm{Mn^{II}(L)_2}]^{2+}$ (L = terpy (2,2′:6′,2″-terpyridine) and ^{t}Bu$_3$-terpy (4,4′,4″-tritert-butyl-2,2′:6′,2″-terpyridine)), has been investigated in dry CH$_3$CN. Under these conditions, the cyclic voltammograms of these complexes exhibit not only the well-known Mn^{II}/Mn^{III} oxidation system but also a second metal-based oxidation one, corresponding to the Mn^{III}/Mn^{IV} redox couple. These oxidative processes are located at $E_{1/2} = +0.96$ and $+1.77$ V vs Ag/Ag$^+$ ($+1.26$ and $+2.07$ V vs SCE) for the terpy complex and $E_{1/2} = +0.85$ and $+1.56$ V vs Ag/Ag$^+$ ($+1.15$ and $+1.86$ V vs SCE) for the ^{t}Bu$_3$-terpy derivative. The one-electron oxidized form of these complexes, $[\mathrm{Mn^{III}(L)_2}]^{3+}$, has been quantitatively generated by exhaustive electrolyses at $E = 1.30$ V, as previously observed in the case of the oxidation of $[\mathrm{Mn^{II}(tolyl\text{-}terpy)_2}]^{2+}$ (tolyl-terpy = 4′-(4-Methylphenyl)-2,2′:6′,2″-terpyridine) (Romain, S.; Duboc, C.; Neese, F.; Rivière, E.; Hanton, L. R.; Blackman, A. G.; Leprêtre, J.-C.; Deronzier, A.; Collomb, M.-N. *Chem.—Eur. J.* **2009**, *15*, 980−988). Further electrolyses at $E = 1.65$−1.80 V of $[\mathrm{Mn^{III}(L)_2}]^{3+}$ solutions have shown that the $[\mathrm{Mn^{IV}(L)_2}]^{4+}$ species is only stable for L = ^{t}Bu$_3$-terpy because of the strong electron-donating properties of the *tert*-butyl substituents. These electrogenerated high-valent complexes are rare examples of mononuclear Mn^{III} and Mn^{IV} complexes stabilized solely by neutral N ligands. They have been fully characterized in solution by UV−visible and electron paramagnetic resonance (EPR) spectroscopies. A detailed investigation of the EPR spectra of the $[\mathrm{Mn^{II}(^{t}Bu_3\text{-}terpy)_2}]^{2+}$ and $[\mathrm{Mn^{IV}(^{t}Bu_3\text{-}terpy)_2}]^{4+}$ has allowed the determination of the spin Hamiltonian parameters for both systems (for Mn^{II}: $|D| = 0.059$ cm^{-1}; $|E| = 0.014$ cm^{-1}; $E/D = 0.259$; $g_x = g_y = g_z = 2.00$ and for Mn^{IV}: $|D| = 1.33(6)$ cm^{-1}; $|E| = 0.36(4)$ cm^{-1}; $E/D = 0.27$; $g_x = 1.96(4)$; $g_y = 1.97(4)$; $g_z = 1.98(4)$).

Introduction

The coordination chemistry of manganese(III) and manganese(IV) has been increasingly studied in an effort to mimic the biological systems that contain or go through these oxidation states during their catalytic cycles.[1] This is particularly true for the oxygen evolving complex (OEC) of photosystem II, which plays the important role of oxidizing water to dioxygen via an oxo-bridged tetranuclear manganese cluster.[2]

Most of the manganese complexes isolated at these high valent oxidation states are multinuclear, the dominant

---

[*] To whom correspondence should be addressed. E-mail: marie-noelle.collomb@ujf-grenoble.fr.

[†] Current Address: Laboratoire de Bioénergétique et Ingénierie des Protéines, CNRS, Université de Provence, Marseille, France.

[‡] Current Address: LEPMI/ELSA/ENSEEG, Domaine Universitaire, 1130 rue de la piscine, BP 75, 38042 Saint Martin d'Hères, France.

(1) (a) Wu, J.; Penner-Hahn, J. E.; Pecoraro, V. L *Chem. Rev* **2004**, *104*, 903, and references therein. (b) Mukhopadhyay, S.; Mandal, S. K.; Bhaduri, S.; Armstrong, W. H. *Chem. Rev.* **2004**, *104*, 3981, and references therein.

(2) (a) Barber, J.; Murray, J. W. *Coord. Chem. Rev.* **2008**, *252*, 233. (b) Dau, H.; Haumann, M. *Coord. Chem. Rev.* **2008**, *252*, 273. (c) Mullins, C. S.; Pecoraro, V. L. *Coord. Chem. Rev.* **2008**, *252*, 416. (d) Cady, C. W.; Crabtree, R. H.; Brudvig, G. W. *Coord. Chem. Rev.* **2008**, *252*, 444. (e) Barber, J. *Inorg. Chem.* **2008**, *47*, 1700. (f) Pecoraro, V. L.; Hsieh, W.-Y. *Inorg. Chem.* **2008**, *47*, 1765. (g) Tagore, R.; Crabtree, R. H.; Brudvig, G. W. *Inorg. Chem.* **2008**, *47*, 1815.

(3) (a) Weatherburn, D. C.; Mandal, S.; Mukhopadhyay, S.; Bahduri, S.; Lindoy, L. F. Manganese. In *Comprehensive Coordination Chemistry II*; McCleverty, J. A., Meyer, T. J., Eds.; Elsevier Pergamon: Oxford, 2004; Vol. *5*, p 1. (b) Collomb, M.-N.; Deronzier, A. Manganese Inorganic & Coordination Chemistry. In *Encyclopedia of Inorganic Chemistry*, 2nd ed.; King R. B., Ed.; Wiley: New York, 2005; p 2894.

10.1021/ic8024342 CCC: $40.75

Scheme 1. Redox Processes Observed in $\mathrm{Mn^{II}}$-bis-terpyridyl Complexes in Dry CH_3CN

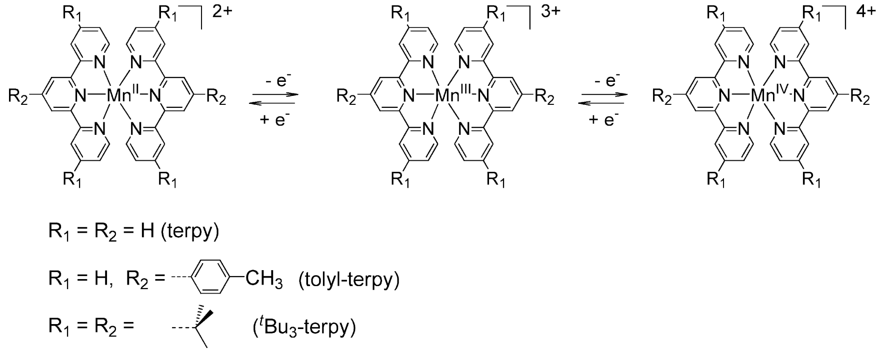

forms consisting of oxo, alkoxo, and carboxylato bridged di-, tri-, and tetranuclear.[1,3] The stabilization of these polynuclear forms is due to the strong electronegative donor properties of the oxygen ligands. In contrast, the number of isolated mononuclear manganese complexes is more limited, (especially in the $\mathrm{Mn^{IV}}$ state) and these compounds are generally stabilized by strong anionic donor ligands (O/S/N ligands, halides or pseudohalides).[1,2c,3,4] Few mononuclear $\mathrm{Mn^{III}}$,[5] and $\mathrm{Mn^{IV}}$,[6] complexes coordinated solely by N ligands were isolated, and only the sarcophagine complexes $[\mathrm{Mn^{III}(sar)}](\mathrm{NO_3})_3$[5j] and $[\mathrm{Mn^{III}((NH_3)_2sar)}](\mathrm{NO_3})_5$ (sar = 3,6,10,13,16,19-hexaazabicyclo[6.6.6]icosane; $(\mathrm{NH_3})_2$sar = 1,8-diamino-sar)[5k] and the biguanide complexes, $[\mathrm{Mn^{III}\{C_2H_4(bigH)_2\}}](\mathrm{NO_3})_3$,[5l] and $[\mathrm{Mn^{IV}(bigH)_3}]^{4+}$,[6d−f] (bigH = $C_2N_5H_7$) are in a neutral environment. We recently reported the isolation of an additional example of such compounds with polypyridyl ligands, namely, $[\mathrm{Mn^{III}(tolyl\text{-}terpy)_2}]^{3+}$ (tolyl-terpy = 4′-(4-Methylphenyl)-2,2′:6′,2″-terpyridine), prepared by an electrochemical oxidation of $[\mathrm{Mn^{II}(tolyl\text{-}terpy)_2}]^{2+}$ in dry CH_3CN medium.[7] The structure of this $\mathrm{Mn^{III}}$ complex was resolved by X-ray analysis of single crystals afforded by an electrocrystallization procedure, and its physical properties were determined. Therefore, this last study provided the first example of a stable mononuclear $\mathrm{Mn^{III}}$ containing only polypyridinyl ligands. Prior to this work, it was proposed that this kind of mononuclear $\mathrm{Mn^{III}}$ complexes was instable because of its high propensity to form high-valent oxo bridged binuclear complexes in the presence of water.[8]

In this Article, we explore the possibilities to electrogenerate these $[\mathrm{Mn^{III}(L)_2}]^{3+}$ species with L = terpy and ^{t}Bu$_3$-terpy (4,4′,4″-tritert-butyl-2,2′:6′,2″-terpyridine) by an oxidation of the corresponding $\mathrm{Mn^{II}}$ complexes in strictly anhydrous CH_3CN medium (Scheme 1). More importantly, we will see that polypyridyl $[\mathrm{Mn^{IV}(L)_2}]^{4+}$ mononuclear species can be electrochemically accessible.

The spectroscopic characteristics (X-band electron paramagnetic resonance (EPR) and UV−visible) of these electrogenerated mononuclear $\mathrm{Mn^{III}}$ and $\mathrm{Mn^{IV}}$ complexes in solution are also described. Although EPR spectroscopy is routinely used to identify mononuclear $\mathrm{Mn^{IV}}$ complexes, a precise determination of the electronic parameters of the $\mathrm{Mn^{IV}}$ ion is rarely found in literature.[4d,h,9]

Experimental Section

General Procedures. Tetrabutylammonium perchlorate (Bu_4NClO_4) (Fluka, puriss, electrochemical grade) and acetonitrile (CH_3CN, Rathburn, HPLC grade) were used as received and stored under an argon atmosphere in a glovebox. The ligands 2,2′:6′,2″-terpyridine (terpy, 99.9%, Alfa Aesar), 4,4′,4″-tritert-butyl-2,2′:

---

(4) See for examples of mononuclear $\mathrm{Mn^{IV}}$ complexes: (a) Chin, D.-H.; Sawyer, D. T.; Schaeffer, W. P.; Simmons, C. J *Inorg. Chem.* **1983**, *22*, 752. (b) Hartman, J. R.; Foxman, B. M.; Cooper, S. R. *Inorg. Chem.* **1984**, *23*, 1381. (c) Sheriff, T. S.; Carr, P.; Coles, S. J.; Hursthouse, M. B.; Lesin, J.; Light, M. E. *Inorg. Chim. Acta* **2004**, *357*, 2494. (d) Parsell, T. H.; Behan, R. K.; Green, M. T.; Hendrich, M. P.; Borovik, A. S. *J. Am. Chem. Soc.* **2006**, *128*, 8728. (e) Dutta, S.; Basu, P.; Chakravorty, A. *Inorg. Chem.* **1991**, *30*, 4031. (f) Pradeep, C. P.; Zacharias, P. S.; Das, S. K. *Polyhedron* **2005**, *24*, 1410. (g) Rajendiran, T. M.; Kampf, J. W.; Pecoraro, V. L. *Inorg. Chim. Acta* **2002**, *339*, 497. (h) Weyhermüller, T.; Paine, T. K.; Bothe, E.; Bill, E.; Chaudhuri, P. *Inorg. Chim. Acta* **2002**, *337*, 344. (i) Min, K. S.; Weyhermüller, T.; Wieghardt, K. *Dalton Trans.* **2004**, 178. (j) Mukhopadhyay, R.; Bhattacharjee, S.; Pal, C. K.; Karmakar, S.; Bhattacharyya, R. *J. Chem. Soc., Dalton Trans.* **1997**, 2267. (k) Koikawa, M.; Okawa, H. *J. Chem. Soc., Dalton Trans.* **1988**, 641.

(5) Mononuclear $\mathrm{Mn^{III}}$ complexes with only N ligands:(a) Ellison, J. J.; Power, P. P.; Shoner, S. C. *J. Am. Chem. Soc.* **1989**, *111*, 8044. (b) Cummins, C. C.; Lee, J.; Schrock, R. R.; Davis, W. M. *Angew. Chem., Int. Ed. Engl.* **1992**, *31*, 1510. (c) Gregory, D. H.; Barker, M. G.; Edwards, P. P.; Siddons, D. J. *Inorg. Chem.* **1995**, *34*, 5195. (d) Sim, P. G.; Sinn, E. *J. Am. Chem. Soc.* **1981**, *103*, 241. (e) de Bruin, B.; Bill, E.; Bothe, E.; Weyhermüller, T.; Wieghardt, K. *Inorg. Chem.* **2000**, *39*, 2936. (f) Limburg, J.; Vrettos, J. S.; Crabtree, R. H.; Brudvig, G. W.; de Paula, J. C.; Hassan, A.; Barra, A.-L.; Duboc-Toia, C.; Collomb, M.-N. *Inorg. Chem.* **2001**, *40*, 1698. (g) Mantel, C.; Hassan, A.; Pécaut, J.; Deronzier, A.; Collomb, M.-N.; Duboc-Toia, C. *J. Am. Chem. Soc.* **2003**, *125*, 12337. (h) Meyer, K.; Bendix, J.; Metzler-Nolte, N; Weyhermuller, T.; Wieghardt, K. *J. Am. Chem. Soc.* **1998**, *120*, 7260. (i) Hubin, T. J.; McCormick, J. M.; Alcock, N. W.; Busch, D. H. *Inorg. Chem.* **2001**, *40*, 435. (j) Anderson, P. A.; Creaser, I. I.; Dean, C.; Harrowfield, J. M.; Horn, E.; Martin, L. L.; Sargeson, A. M.; Snow, M. R.; Tiekink, E. R. T. *Aust. J. Chem.* **1993**, *46*, 449. (k) Creaser, I. I.; Engelhardt, L. M.; Harrowfield, J. M.; Sargeson, A. M.; Skelton, B. W.; White, A. H. *Aust. J. Chem.* **1993**, *46*, 465. (l) De, A. *Acta Crystallogr.* **1990**, *C46*, 1004.

(6) Mononuclear $\mathrm{Mn^{IV}}$ complexes with only N ligands:(a) Chan, M. K.; Armstrong, W. H. *Inorg. Chem.* **1989**, *28*, 3779. (b) Dave, B. C.; Czernuszewicz, R. S. *J. Coord. Chem.* **1994**, *33*, 257. (c) Hart, R. O. C.; Bott, S. G.; Atwood, J. L.; Cooper, S. R. *J. Chem. Soc., Chem. Commun.* **1992**, 894. (d) Das, G.; Bharadwaj, P. K.; Ghosh, D.; Chaudhuri, B.; Banerjee, R. *Chem. Commun.* **2001**, 323. (e) Lu, L.-P.; Zhu, M.-L.; Yang, P. *Acta Crystallogr.* **2004**, *C60*, m18. (f) Das, A.; Mukhopadhyay, S.; Lu, L. P.; Zhu, M.-L. *J. Chem. Crystallogr.* **2006**, *36*, 297.

(7) Romain, S.; Duboc, C.; Neese, F.; Rivière, E.; Blackman, A.; Leprêtre, J.-C.; Deronzier, A.; Collomb, M.-N. *Chem.—Eur. J.* **2009**, *15*, 980–988.

6′,2″-terpyridine ($^tBu_3$-terpy, 98%, Aldrich) were used as received. The complex $[Mn(^tBu_3\text{-terpy})_2](PF_6)_2$ was prepared as previously described.[10]

Synthesis of $[Mn^{II}(terpy)_2](ClO_4)_2$. A solution of terpy (0.248 g, 1.06 mmol) in ethanol (50 mL) was added to a stirred solution of $Mn(ClO_4)_2 \cdot 6H_2O$ (0.159 g, 0.44 mmol) in ethanol (5 mL). The resulting yellow solution was heated to reflux during 1 h. After cooling to room temperature, the complex precipitated as a yellow powder. The powder was filtered off, washed with ethanol and then with diethyl ether. Yield: 0.260 g (82%). Elemental anal. Calcd: $C_{30}H_{22}MnN_6O_8Cl_2 \cdot H_2O$ (738.39): C 48.79, H 3.28, N 11.38. Found: C 48.74, H 2.98, N 11.33. ESI-MS: *m/z* (%) 619.91 (10) $[M - ClO_4]^+$, 260.61 (100) $[M - 2ClO_4]^{2+}$. **Caution!** *Perchlorate salts of compounds containing organic ligands are potentially explosive. Although we have encountered no such problems, only small quantities of these compounds should be prepared and handled with care.*

Electrochemistry. All electrochemical measurements were made under an argon atmosphere in a dry-glovebox at room temperature. Cyclic voltammetry and controlled potential electrolysis experiments were performed using an EG&G model 173 potentiostat/galvanostat equipped with a PAR model universal programmer and a PAR model 179 digital coulometer. A standard three-electrode electrochemical cell was used. Potentials were referred to an Ag/0.01 M $AgNO_3$ reference electrode in CH_3CN + 0.1 M Bu_4NClO_4. Potentials referred to that system can be converted to the ferrocene/ferricinium couple by subtracting 87 mV, to SCE by adding 298 mV, or to the NHE reference electrode by adding 0.548 V. The working electrodes were platinum disks polished with 2 μm diamond paste (Mecaprex Presi). They were 5 mm in diameter for cyclic voltammetry (E_{pa}, anodic peak potential; E_{pc}, cathodic peak potential; $E_{1/2} = (E_{pa} + E_{pc})/2$; $\Delta E_p = E_{pa} - E_{pc}$) and 2 mm in diameter for rotating disk electrode experiments (RDE). Exhaustive electrolyses were carried out on a reticulated vitreous carbon electrode 45 PPI (the electrosynthesis Co. Inc., 1 cm^3). The auxiliary electrode was a Pt wire in CH_3CN + 0.1 M Bu_4NClO_4.

Spectroscopies. For electrochemical experiments, electronic absorption spectra were recorded on a Varian Cary 50 or 100 absorption spectrophotometer. Initial and electrolyzed solutions were transferred to conventional 0.1 or 1 cm path length quartz cells in the glovebox. X-band electronic paramagnetic resonance (EPR, 9.4 GHz) spectra were recorded with a Bruker ESP 300 E spectrometer for the 100 K experiments and with a Bruker EMX, equipped with an Oxford Instruments ESR-900 continuous-flow helium cryostat and an ER-4116 DM Bruker cavity for the 4.5 K experiments.

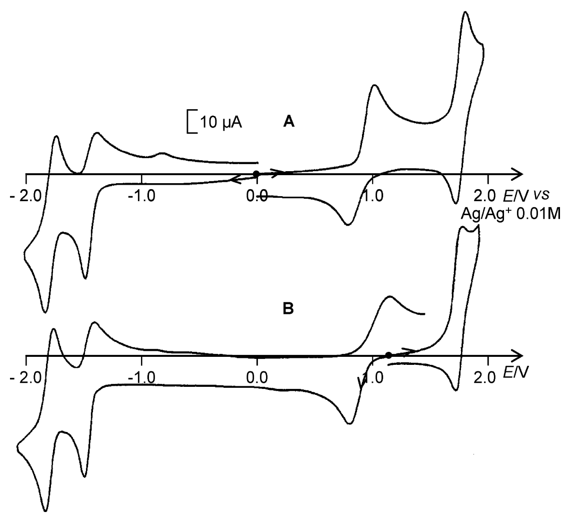

Figure 1. Cyclic voltammograms of a 0.83 mM solution of $[Mn^{II}(terpy)_2]^{2+}$ in CH_3CN + 0.1 M Bu_4NClO_4 at a Pt electrode (A); after an exhaustive oxidation at 1.30 V (formation of $[Mn^{III}(terpy)_2]^{3+}$) (B); v = 100 mV s^{-1}.

Results and Discussions

Electrochemical Behavior. Electrochemical oxidation of manganese(II) polypyridyl complexes $[Mn^{II}(L)_3]^{2+}$ with bidentate ligands (L = bpy, phen) in CH_3CN is known to lead to the mixed-valent di-μ-oxo bridged binuclear complexes $[Mn^{III,IV}(O)_2(L)_4]^{3+}$.[8a−f] The dimerization process is complicated and is believed to be due to the instability of the corresponding $[Mn^{III}(L)_3]^{3+}$ species that disproportionate by reacting with residual water present in the solvent, thereby releasing one N-ligand to form oxo bridges.[8a] For terpyridine complexes, the final oxidation products of $[Mn^{II}(L)_2]^{2+}$ (L = terpyridine substituted or not) in CH_3CN remained unidentified (until our recent work on the tolyl-terpy derivative)[7] except when the oxidation is achieved in the presence of coordinating anions like $CF_3CO_2^-$.[8g] In this case, the quantitative formation of a μ-oxo dinuclear complex $[Mn_2^{III,IV}O_2(terpy)_2(CF_3CO_2)_2]^+$ was obtained. In pure aqueous solutions, the same dimerization process occurs, leading to the quantitative generation of $[Mn_2^{III,IV}O_2(L)_2]^{3+}$,[8h−j] (L = bpy, phen) and $[Mn_2^{III,IV}O_2(terpy)_2(H_2O)_2]^{3+}$, respectively.[8l] A further oxidation of these mixed-valent complexes is followed by a second dimerization process by formation of additional oxo bridges, in that way conducting to the linear tetranuclear complexes, $[Mn_4^{IV}O_6(L)_6]^{4+}$,[8h−j] and $[Mn_4^{IV}O_5(terpy)_4(H_2O)_2]^{6+}$.[8l]

As pointed out above, we recently reported that the Mn^{III} species $[Mn^{III}(tolyl\text{-}terpy)_2]^{3+}$ can be obtained by an electrochemical oxidation of $[Mn^{II}(toly{-}terpy)_2]^{2+}$ in dry CH_3CN, the dimerization process being avoided in these experimental conditions.[7]

Figures 1 and 2 show the cyclic voltammograms of the terpy and $^tBu_3$-terpy complexes obtained in the same dry conditions. They display, as previously reported for bis-terpyridine complexes (L = terpy, 4′-X-terpy (*X* = Cl,

---

(8) (a) Morrison, M. M.; Sawyer, D. T. *Inorg. Chem.* **1978**, *17*, 333. (b) Dunand-Sauthier, M.-N. C.; Deronzier, A.; Moutet, J.-C.; Tingry, S. *J. Chem. Soc., Dalton Trans.* **1996**, 2503. (c) Dunand-Sauthier, M.-N. C.; Deronzier, A. *J. Electroanal. Chem.* **1997**, *428*, 65. (d) Baffert, C.; Dumas, S.; Chauvin, J.; Leprêtre, J.-C.; Collomb, M.-N.; Deronzier, A. *Phys. Chem. Chem. Phys.* **2005**, *7*, 202. (e) Romain, S.; Baffert, C.; Dumas, S.; Chauvin, J.; Leprêtre, J.-C.; Daveloose, D.; Deronzier, A.; Collomb, M.-N. *Dalton Trans.* **2006**, 5691. (f) Romain, S.; Leprêtre, J.-C.; Chauvin, J.; Deronzier, A.; Collomb, M.-N. *Inorg. Chem.* **2007**, *46*, 2735. (g) Baffert, C.; Collomb, M.-N.; Deronzier, A.; Pécaut, J.; Limburg, J.; Crabtree, R. H.; Brudvig, G. W. *Inorg. Chem.* **2002**, *41*, 1404. (h) Dunand-Sauthier, M.-N. C.; Deronzier, A.; Pradon, X.; Ménage, S.; Philouze, C. *J. Am. Chem. Soc.* **1997**, *119*, 3173. (i) Dunand-Sauthier, M.-N. C.; Deronzier, A.; Piron, A.; Pradon, X.; Ménage, S. *J. Am. Chem. Soc.* **1998**, *120*, 5373. (j) Dunand-Sauthier, M.-N. C.; Deronzier, A.; Piron, A. *J. Electroanal. Chem.* **1999**, *463*, 119. (k) Collomb, M.-N.; Deronzier, A.; Richardot, A.; Pécaut, J. *New J. Chem.* **1999**, *23*, 351. (l) Baffert, C.; Romain, S.; Richardot, A.; Leprêtre, J.-C.; Lefebvre, B.; Deronzier, A.; Collomb, M.-N. *J. Am. Chem. Soc.* **2005**, *127*, 13694. (m) Collomb, M.-N.; Deronzier, A. *Eur. J. Inorg. Chem.*,accepted for publication.

(9) (a) Camenzind, M. J.; Hollander, F. J.; Hill, C. L. *Inorg. Chem.* **1983**, *22*, 3776. (b) Duboc-Toia, C.; Hummel, H.; Bill, E.; Barra, A.-L.; Chouteau, G.; Wieghardt, K. *Angew. Chem., Int. Ed.* **2000**, *39*, 2888.

(10) Duboc, C.; Collomb, M.-N.; Pécaut, J.; Deronzier, A.; Neese, F. *Chem.—Eur. J.* **2008**, *14*, 6498.

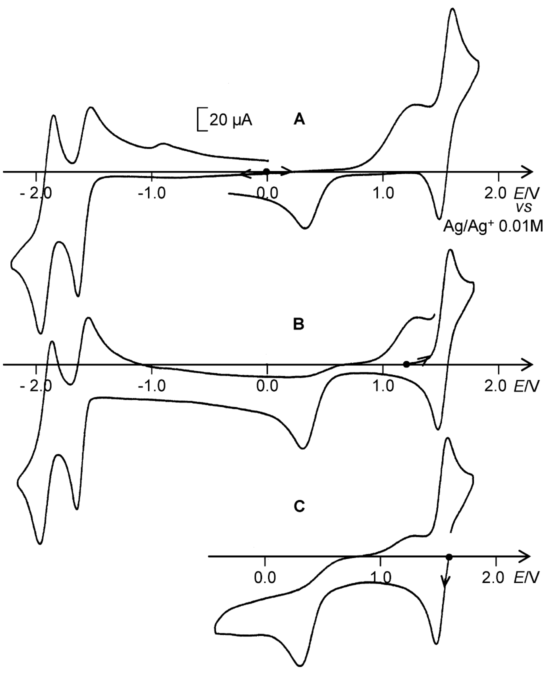

Figure 2. Cyclic voltammograms of a 1.75 mM solution of $[Mn^{II}(^{t}Bu_3\text{-terpy})_2]^{2+}$ in CH_3CN + 0.1 M Bu_4NClO_4 at a Pt electrode (A); after an exhaustive oxidation at 1.30 V (formation of $[Mn^{III}(^{t}Bu_3\text{-terpy})_2]^{3+}$) (B); after an exhaustive oxidation at 1.65 V (formation of $[Mn^{IV}(^{t}Bu_3\text{-terpy})_2]^{4+}$) (B); $v = 100$ mV s^{-1}.

CH_3−Ph (tolyl), OH, pyrr (pyrr = pyrrolidine) and 4,4′,4″-Ph_3-terpy),[7,8a,g,11] two successive one-electron ligand-centered reversible reduction processes and a metal-based oxidation process, Mn^{II}/Mn^{III}, more or less reversible, located at $E_{1/2} = +0.96$ V vs Ag/Ag^+ (+1.26 V vs SCE) for terpy and $E_{1/2} = +0.85$ V (1.15 V vs SCE) for $^{t}Bu_3$-terpy (Table 1). In these anhydrous conditions, we also evidence that, by scanning at lower negative potential and higher positive potential, it is possible to observe a third reduction system assigned to the second reduction of one terpyridine ligand (Table 1) and a second one-electron metal-centered reversible oxidation process, Mn^{III}/Mn^{IV}. This second wave is located at $E_{1/2} = +1.77$ V vs Ag/Ag^+ (+2.07 vs SCE) for terpy and $E_{1/2} = +1.56$ V (+1.86 vs SCE) for $^{t}Bu_3$-terpy (Figures 1 and 2, Table 1). The existence of this second process has been only very recently reported for the tolyl-terpy[7] and the 4′-pyrr-terpy[11d] complexes. For this latter complex, the strong electron-donating properties of the pyrrolidine substituent shift by 0.3−0.5 V to lower potential compared to the unsubstituted terpy complex (Table 1). Despite the donor effect of the three *tert*-butyl substituents for the $^{t}Bu_3$-terpy complex, the shift to lower potential is less pronounced than for the 4′-pyrr-terpy complex.

For the terpy and tolyl-terpy complexes, the ΔE_p ($\Delta E_p = E_{pa} - E_{pc}$) value of the Mn^{II}/Mn^{III} system varying from 80 to 930 mV is strongly dependent on the etching of the electrode surface, the scan rate, and the potential limit used. For the $^{t}Bu_3$-terpy, the ΔE_p value remains always high, ranging between 480 (at 20 mVs^{-1}) and 980 mV (at 100 mVs^{-1}), and does not depend on the experimental conditions (Figure 2A). Different hypotheses can explain this phenomenon: (i) a poor contact between the complex and the electrode surface because of the large size of the ligands, (ii) the electrode poisoning induced by adsorption of the complex coupled to the electron transfer, as suggested by Hughes et al.,[11a,b] and (iii) the expected Jahn−Teller distortion that occurs with oxidation to Mn^{III} as suggested by Un et al.[11d] In contrast, the reversibility of the second oxidation system Mn^{III}/Mn^{IV} does not depend on the experimental conditions. Indeed, the ΔE_p for the three complexes remains below 100 mV for scan rates ranging between 20 and 200 mVs^{-1}.

Rotating disk electrode (RDE) experiments have been carried out to verify the number of electron exchanged for each of the reversible redox processes (two oxidative and two reductive ones). It appears that the height of the four redox processes is identical, confirming that each process corresponds to the exchange of one-electron (panels A and B of Figure 3, curves (a)).

Exhaustive electrolyses of dry CH_3CN solutions of $[Mn^{II}(L)_2]^{2+}$ (L = terpy, $^{t}Bu_3$-terpy) have been carried out at room temperature to evaluate their stabilities at the +III and +IV oxidation states. An oxidation at $E = 1.30$ V consumed one electron per molecule of initial complex and leads to the formation of orange solutions of $[Mn^{III}(L)_2]^{3+}$. Because of the strong electron donor properties of the *tert*-butyl substituents, electrogenerated solutions of $[Mn^{III}(^{t}Bu_3\text{-terpy})_2]^{3+}$ are stable for several weeks, while solutions of $[Mn^{III}(\text{terpy})_2]^{3+}$ less than 1 h. Indeed, despite the use of dry CH_3CN and electrolyte, the presence of residual water cannot be completely avoided, and is in a sufficient amount for inducing slow disproportionation of the complex to form oxo-bridged multinuclear species. A detailed electrochemical study related to the formation of such complexes is currently underway. The quantitative formation of $[Mn^{III}(\text{terpy})_2]^{3+}$ is obtained by the use of a large surface working electrode based on reticulated vitreous carbon, which minimizes the time of electrolysis to about 5−10 min. An exhaustive electrolysis carried out on a platinum plate takes more than 1 h and leads to the partial transformation of the Mn^{III} complex into oxo bridged species. In contrast to $[Mn^{III}(\text{tolyl-terpy})_2]^{3+}$ that progressively precipitates during the electrolysis,[7] the resulting terpy and $^{t}Bu_3$-terpy Mn^{III} complexes are fully soluble in CH_3CN + 0.1 M Bu_4NClO_4 even at concentrations higher than 5 mM. The cyclic voltammograms of the electrogenerated solutions (Figures 1B and 2B) are similar to that of $[Mn^{III}(\text{tolyl-terpy})_2]^{3+}$ obtained after redissolution in CH_3CN + 0.05 M Bu_4NBF_4,[7] where the compound is more soluble. The voltammograms at RDE before and after electrolyses are in accordance with the quantitative formation of the Mn^{III} complexes (panels A and B of Figure 3, curves (b)). It should be noted that for the $^{t}Bu_3$-terpy complex, the ΔE_p value (E_{pa}= 1.40 V and

---

(11) (a) Rao, J. M.; Hughes, M. C.; Macero, D. J. *Inorg. Chim. Acta* **1976**, *18*, 127. (b) Hughes, M. C.; Macero, D. J.; Rao, J. M. *Inorg. Chim. Acta* **1981**, *49*, 241. (c) Gätjens, J.; Sjödin, M.; Pecoraro, V. L.; Un, S. *J. Am. Chem. Soc.* **2007**, *129*, 13825. (d) Sjödin, M.; Gätjens, J.; Tabares, L. C.; Thuéry, P.; Pecoraro, V. L.; Un, S. *Inorg. Chem.* **2008**, *47*, 2897.

Table 1. Electrochemical Data for $[Mn^{II}(L)_2]^{2+}$ in Anhydrous CH_3CN + 0.1 M Bu_4NClO_4 vs Ag/Ag^+ (0.01 M $AgNO_3$ in CH_3CN + 0.1 M Bu_4NClO_4), at a Scan Rate of 100 mV s^{-1}

	oxidation processes		reduction processes[a]		
	$E_{1/2}$/V (ΔE_p/mV)		$E_{1/2}$/V (ΔE_p/mV)		
complexes	Mn^{III}/Mn^{II}	Mn^{IV}/Mn^{III}	1st	2nd	3th
$[Mn(terpy)_2]^{2+}$	0.96 (80)	1.77 (100)	−1.42 (80)	−1.76 (80)	−2.27 (140)[c]
$[Mn(tolyl\text{-}terpy)_2]^{2+,b,7}$	0.91 (80)	1.63 (100)	−1.43 (80)	−1.70 (120)	−2.19 (180)[c]
$[Mn(^tBu_3\text{-}terpy)_2]^{2+}$	0.85 (480)[b]	1.56 (80)	−1.58 (90)	−1.90 (80)	−2.41 (100)[c]
$[Mn(4'\text{-}pyrr\text{-}terpy)_2]^{2+,11d}$	0.50 (108)	1.22	−1.84	−1.99	

[a] The oxidation system is poorly reversible and the potential given corresponds to the E_{pa} value. [b] In CH_3CN + 0.05 M Bu_4NBF_4. [c] The determination of the $E_{1/2}$ of this system which corresponds to the second reduction of one terpyridine ligand is inaccurate because of the proximity of the solvent reduction.

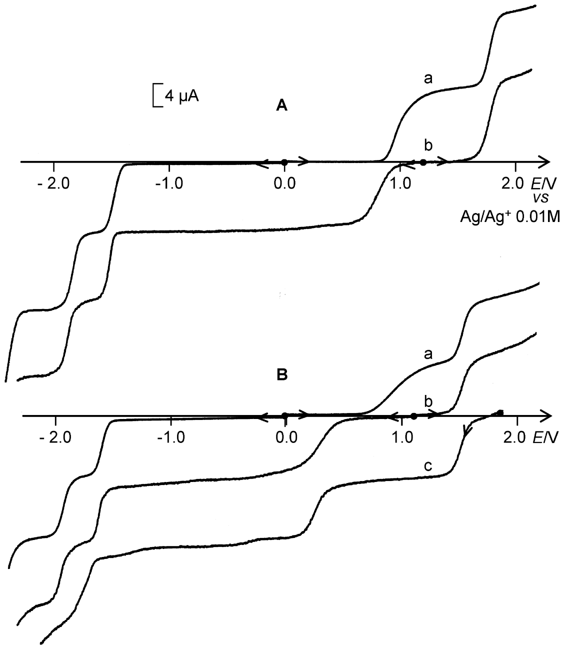

Figure 3. Voltammograms at a Pt RDE at ω = 600 tr min^{-1} (v = 10 mV s^{-1}) in CH_3CN + 0.1 M Bu_4NClO_4 of (A) a 0.83 mM solution of $[Mn^{II}(terpy)_2]^{2+}$ in CH_3CN + 0.1 M Bu_4NClO_4 (a), after exhaustive oxidation at 1.30 V (b); (B) a 0.80 mM solution of $[Mn^{II}(^tBu_3\text{-}terpy)_2]^{2+}$ (a), after exhaustive oxidation at 1.30 V (b), after exhaustive oxidation at 1.65 V (c).

E_{pc}= 0.44 V) of the Mn^{II}/Mn^{III} system remains very high (Figures 2B and 3B).

These oxidation processes are associated by significant changes in UV−visible absorption spectroscopy (Table 2 and Figures 4 and 5). The $[Mn^{II}(L)_2]^{2+}$ complexes present bands only in the near UV region assigned to the $\pi \rightarrow \pi^*$ bands of the ligand, whereas the orange solutions of $[Mn^{III}(L)_2]^{3+}$ are dominated by Mn^{III} d-d transitions at around 455, 360, and 320 nm. These visible Mn^{III} spectra are in close correspondence to that of $[Mn^{III}(tolyl\text{-}terpy)_2]^{3+}$.[7]

The tertio-butyl substituents also allow the better stabilization of the +IV oxidation state. Indeed, an exhaustive electrolysis at 1.65 V of an electrogenerated solution of $[Mn^{III}(^tBu_3\text{-}terpy)_2]^{3+}$ leads to the formation of $[Mn^{IV}(^tBu_3\text{-}terpy)_2]^{4+}$, after the consumption of one additional electron.[12] The comparison of the waves height of the RDE voltammograms before and after electrolysis shows that this Mn^{IV} complex is formed with a quasi-quantitative yield (>95%) (Figures 2C and 3B, curve (c)). The UV−visible spectrum of the resulting red solution displays a large intense band at 465 nm and a less intense one at 865 nm attributed to a ligand to metal charge transfer and a d-d transition, respectively (Figure 5A, spectrum (c)). Indeed for octahedral Mn^{IV} complexes, three spin allowed d-d transitions are expected.[4j]

CH_3CN solutions of $[Mn^{IV}(^tBu_3\text{-}terpy)_2]^{4+}$ are, however, not stable over time. Slow transformation of the complex occurs (after less than 1 h) into oxo-bridged multinuclear species. The quantitative formation of $[Mn^{IV}(^tBu_3\text{-}terpy)_2]^{4+}$ by electrolysis depends, as for $[Mn^{III}(terpy)_2]^{3+}$, not only on the use of an anhydrous electrolyte but also on a short electrolysis time. Several attempts to isolate the $[Mn^{IV}(^tBu_3\text{-}terpy)_2]^{4+}$ as a powder sample have failed. The poor stability of $[Mn^{IV}(^tBu_3\text{-}terpy)_2]^{4+}$ is the consequence of its very high reduction potential of $E_{1/2}$ = +1.86 vs SCE. To our knowledge, this complex has the highest Mn^{IV}/Mn^{III} reduction potential among mononuclear complexes which have been isolated in their Mn^{IV} forms (potential comprised in the large range of values of −0.9 to +1.35 V vs SCE).[4,6] The previous highest one (+1.35 V vs SCE) was the structurally characterized pyrazolylborate complex $\{Mn^{IV}[HB(3,5\text{-}Me_2pz)_3]_2\}^{2+}$;[6a] its potential is 0.5 V lower compared to that of $[Mn^{IV}(^tBu_3\text{-}terpy)_2]^{4+}$.

EPR Spectroscopy. These oxidation processes are also monitored by X-band EPR spectroscopy. Upon exhaustive oxidation at 1.30 V, the EPR signal of the initial Mn^{II} complexes at 100 K fully disappears in accordance with the formation of the X-band EPR silent high-spin Mn^{III} species (S = 2) (see Figure 6b for the $^tBu_3$-terpy derivative). After exhaustive oxidation at 1.65 V, the 100 K EPR spectrum of $[Mn^{IV}(^tBu_3\text{-}terpy)_2]^{4+}$ only presents a low amplitude 6-line signal centered at g = 2 corresponding to a small amount of $[Mn^{II}(CH_3CN)_6]^{2+}$ (less than 5%) coming from the decomposition of the complex.[8d−f] An EPR signal, characteristic of a mononuclear Mn^{IV} species, is obtained for experiments recorded at 4.5 K. We have performed a detailed analysis of the X-band EPR spectra of the Mn^{II} and Mn^{IV} complex for the $^tBu_3$-terpy derivative (see below).

The electronic properties of the high-spin Mn^{II} ($3d^5$) and Mn^{IV} ($3d^3$) ions in their electronic ground-state are characterized by a total electronic spin S = 5/2 and S = 3/2, respectively, with a nuclear spin of I = 5/2. These ions are well described by the following spin-Hamiltonian:

$$H = \beta \mathbf{B} \mathbf{g} S + IAS + D[S_z^2 - 1/3S(S+1)] + E(S_x^2 - S_y^2) \quad (1)$$

---

[12] The $[Mn^{IV}(L)_2]^{4+}$ species with L = terpy and tolyl-terpy are not stable. Attempts to generate such complexes by exhaustive electrolyses of solutions of $[Mn^{II}(L)_2]^{2+}$ or $[Mn^{III}(L)_2]^{3+}$ at E = 1.8−1.9 V have led to the formation of Mn^{IV} oxo bridged species.

Table 2. UV-visible Data for the Bis-terpy $[Mn^{II/III/IV}(L)_2]^{2+/3+/4+}$ Complexes in CH_3CN+ 0.1 M Bu_4NClO_4

complexes	λ/nm (ε/M^{-1} cm^{-1})
$[Mn^{II}(terpy)_2]^{2+}$	266 (17800) 276 (19500) 284 (23100) 323 (30600) 335 (30500)
$[Mn^{III}(terpy)_2]^{3+}$	275 (27500) 323 (24600) 366 (11200) 436 (sh, 2200) 457 (2500) 487 (sh, 2000)
$[Mn^{II}(tolyl\text{-}terpy)_2]^{2+,a,7}$	266 (sh, 35000)) 279 (sh, 47100) 288 (60000) 316 (46600) 325 (sh, 45600) 340 (sh, 33300)
$[Mn^{III}(tolyl\text{-}terpy)_2]^{3+,a,7}$	278 (sh, 42000) 289 (46300) 324 (32200) 344 (sh, 29400) 366 (30200) 450 (7250) 485 (sh, 6000)
$[Mn^{II}({}^tBu_3\text{-}terpy)_2]^{2+}$	268 (27000) 275 (24500) 284 (26000) 321 (37000) 332 (38000)
$[Mn^{III}({}^tBu_3\text{-}terpy)_2]^{3+}$	266 (56400) 320 (26600) 361 (21200) 450 (3200) 478 (sh, 2600)
$[Mn^{IV}({}^tBu_3\text{-}terpy)_2]^{4+}$	266 (78300) 320 (36500) 351 (33000) 465 (11000) 865 (1450)

[a] In CH_3CN + 0.05 M Bu_4NBF_4.

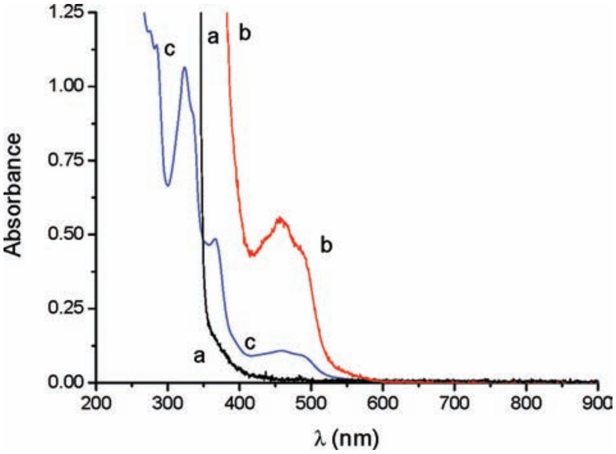

Figure 4. Changes in the UV−visible absorption spectra in CH_3CN + 0.1 M Bu_4NClO_4 of a 2.16 mM solution of $[Mn^{II}(terpy)_2]^{2+}$: (a-black line) initial solution, (b-red line) after exhaustive electrolysis at 1.30 V (formation of $[Mn^{III}(terpy)_2]^{3+}$), (c-blue line) solution of $[Mn^{III}(terpy)_2]^{3+}$ at 0.43 mM; l = 1 mm.

The two first terms represent the Zeeman and electron nuclear hyperfine interactions, respectively, while the last two define the second-order (bilinear) zero field splitting interaction (*zfs*) with D and E being referred to the axial and rhombic parts, respectively. In the case of the Mn^{II} and Mn^{IV} ions, the g anisotropy is low with Landé factors closed to or slightly smaller than $g = 2.00$. Consequently the general profile of an EPR spectrum of mononuclear Mn^{II} and Mn^{IV} complexes is mainly sensitive to the *zfs* terms.

$[Mn^{II}({}^tBu_3\text{-}terpy)_2]^{2+}$ complex. Using multifrequency high field EPR spectroscopy, the *zfs* parameters of the $[Mn^{II}({}^tBu_3\text{-}terpy)_2]^{2+}$ have been precisely determined on powder samples in our previous work.[10] Its X-band EPR signature in frozen CH_3CN solution at 100 K is shown in Figure 7. The *zfs* values determined by simulation of this spectrum ($|D| = 0.059$ cm^{-1}; $|E| = 0.014$ cm^{-1}) differ reasonably compared to those previously published ($|D| = 0.073$ cm^{-1}, $|E| = 0.015$ cm^{-1}). This is ascribed to the high sensitivity of the *zfs* terms to small structural variations (temperature, solid−liquid phases), as previously demonstrated.[10]

$[Mn^{IV}({}^tBu_3\text{-}terpy)_2]^{4+}$ Complex. The 4.5 K EPR spectrum of $[Mn({}^tBu_3\text{-}terpy)_2]^{4+}$ in CH_3CN given in Figure 8 is characterized by large features in the range 800 to 8000 G localized at g = 5.26, 2.46, 2.00, 1.66, and 1.17 (turnover point except for the g = 2 crossover point). The g = 2.00 transition split into a multiplet corresponds to a small amount of $[Mn^{II}(CH_3CN)_6]^{2+}$ as mentioned above. The other signals are the signature of a high-spin mononuclear Mn^{IV} complex.

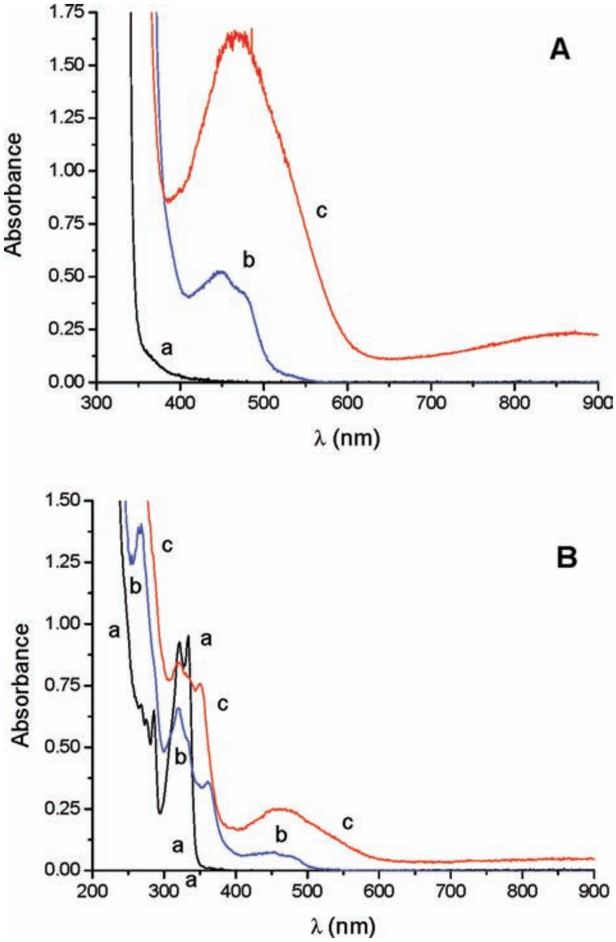

Figure 5. Changes in the UV−visible absorption spectra in CH_3CN + 0.1 M Bu_4NClO_4 of a solution of $[Mn^{II}({}^tBu_3\text{-}terpy)_2]^{2+}$ at 1.65 mM (A) and 0.25 mM (B): (a-black line) initial solution, (b-blue line) after exhaustive electrolysis at 1.30 V (formation of $[Mn^{III}({}^tBu_3\text{-}terpy)_2]^{3+}$), (c-red line) after exhaustive electrolysis at 1.65 V (formation of $[Mn^{IV}({}^tBu_3\text{-}terpy)_2]^{4+}$); l = 1 mm.

It has been shown that the shape of the X-band EPR spectra of $3d^3$ ion depends on the magnitude of D.[13] If $|D|$ is much smaller than the energy provided by the EPR spectrometer $h\nu$ ($D \ll 0.32$ cm^{-1}), the spectrum is dominated by an intense signal at g = 2.00 with other relatively weak features in the low and high field parts. Inversely, if $D \gg 0.32$ cm^{-1} a strong signal in the low field region dominates the spectrum. Its exact field position is correlated to the E/D ratio, from g = 4.1 for a pure axial system (E/D = 0) to g

---

[13] (a) Hempel, J.-C.; Morgan, L. O.; Lewis, W. B. *Inorg. Chem.* **1970**, *9*, 2064. (b) Pederson, E.; Toflund, H. *Inorg. Chem.* **1974**, *13*, 1603.

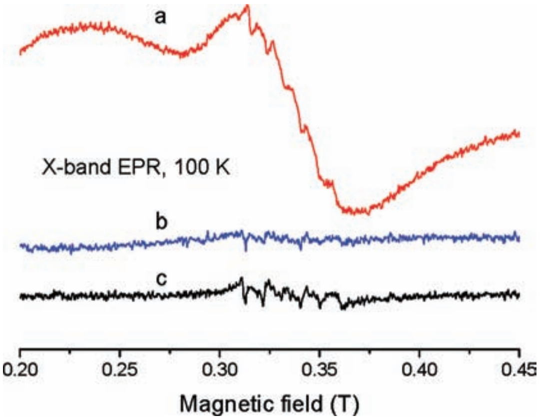

Figure 6. 100 K X-band EPR spectra of a 2.46 mM solution of (a-red line) $[Mn^{II}(^tBu_3\text{-terpy})_2]^{2+}$ in CH_3CN + 0.1 M Bu_4NClO_4 (b-blue line) after exhaustive electrolysis at 1.30 V (formation of $[Mn^{III}(^tBu_3\text{-terpy})_2]^{3+}$) and (c-black line) after exhaustive electrolysis at 1.65 V (formation of $[Mn^{IV}(^tBu_3\text{-terpy})_2]^{4+}$).

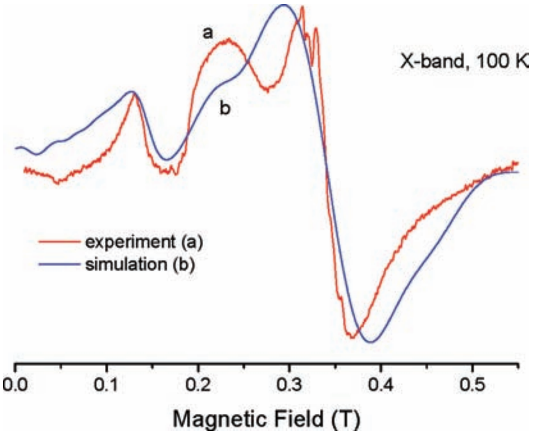

Figure 7. Experimental (a-red) and simulated (b-blue) X-band EPR spectra recorded at 100 K of solution of $[Mn^{II}(^tBu\text{-terpy})_2]^{2+}$ in CH_3CN. Parameters used for the simulation: $|D| = 0.059$ cm^{-1}; $|E| = 0.014$ cm^{-1}; $E/D = 0.259$; $g_x = g_y = g_z = 2.00$.

= 5.5 for a total rhombic system ($E/D = 1/3$). Most of the Mn^{IV} complexes characterized by EPR display a large D value type spectrum. Nevertheless, a precise determination of the magnitude of D is rarely found in the literature.[4d,h,9a]

In the case of $[Mn^{IV}(^tBu_3\text{-terpy})_2]^{4+}$, the intensity and the field position of the $g = 5.26$ signal is the signature of a rhombic system with a large D value. From this g_{eff} value, the E/D ratio can be estimated close to 0.25. This high ratio is in agreement with the expected distorted geometry around the manganese ion imposed by the constrained nature of the tridentate ligand.[7,10,5f,g] The magnitude of the *zfs* parameters was determined by simulating the EPR spectrum using eq 1 that does not take into account the hyperfine interaction. The D value of 1.33 cm^{-1} is close to the few reported D values.[4d,h,9a] The hyperfine coupling constant A, estimated to 67 G from the average separation between two lines of the $g_{eff} = 5.26$ transition, is consistent with a Mn^{IV} species but is lower than that typically observed for such complexes (above 70 G).[4d]

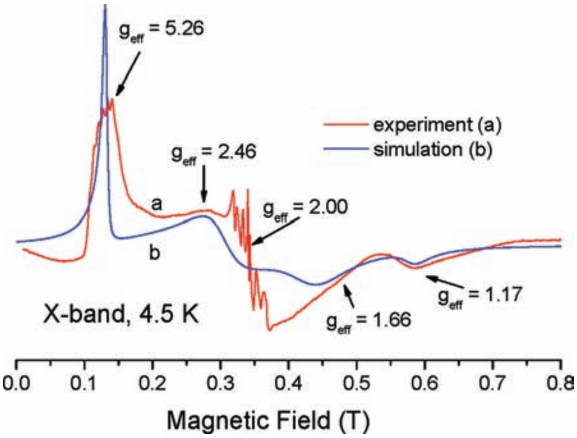

Figure 8. Experimental (a-red) and simulated (b-blue) X-band EPR spectra recorded at 4.5 K of a 3.5 mM solution of $[Mn^{IV}(^tBu\text{-terpy})_2]^{4+}$ in CH_3CN + 0.1 M Bu_4NClO_4. Parameters used for the simulation: $|D| = 1.335$ cm^{-1}; $|E| = 0.36$ cm^{-1}; $E/D = 0.225$; $g_x = 1.96$; $g_y = 1.97$; $g_z = 1.98$.

Conclusion

In summary, in this paper we report the full elucidation of the oxidative electrochemical properties of the mononuclear Mn^{II} bis-terpyridine complexes in CH_3CN. Under dry conditions, two successive metal-based oxidation processes can be observed on the cyclic voltammograms, namely Mn^{II}/Mn^{III} ($E_{1/2} = +1.15$ to $+1.26$ V vs SCE) and Mn^{III}/Mn^{IV} ($E_{1/2} = +1.86$ to $+2.07$ V vs SCE). These high oxidation potentials show that the Mn^{III} or even more the Mn^{IV} level are poorly stabilized by neutral N-ligands as terpyridine. However, in this study we succeeded to electrogenerate and characterize in solution the Mn^{III} level for the terpy and $^tBu_3$-terpy complexes (as previously reported for tolyl-terpy complex) and also the Mn^{IV} level for the $^tBu_3$-terpy derivative. Although these species are more or less stable over time, depending on the terpyridine ligand, their UV−visible and EPR characteristics have been obtained. The +IV oxidation state of the $[Mn(^tBu_3\text{-terpy})_2]^{4+}$ complex has been confirmed by EPR spectroscopy, and its *zfs* terms have been determined, evidencing a rhombic distortion imposed by the two terpyridine ligands.

Finally, these high-valent bis-terpyridine manganese complexes provide rare examples of mononuclear Mn^{III} and Mn^{IV} complexes coordinated solely by neutral N ligands.

Acknowledgment. The authors thank Daniele Limosin for her participation in the electrochemical experiments and the Agence Nationale pour la Recherche (Grant ANR-05-JCJC-0171-01) for financial support.

IC8024342